Implementation of a Digital Directional Fault Passage Indicator

Carlos González de Miguel
ESAT/ELECTA
KU Leuven, Belgium
carlos.gonzalezdemiguel@esat.kuleuven.be

Tom De Rybel
KIC-InnoEnergy
Eindhoven, The Netherlands
tom.derybel@kic-innoenergy.com

Johan Driesen
ESAT/ELECTA
KU Leuven, Belgium
johan.driesen@esat.kuleuven.be

***Abstract*—Fault Passage Indicators (FPIs) are a cost effective solution to increase grid reliability. The connection of Distributed Generation units can lead them to misoperate and undermine the reliability improvements. Directional FPIs is a solution to overcome this problem. In this paper, the fault detection methods and direction-polarization principles for an isolated grid are described. As well, the implementation is done in Matlab-Simulink, from the signal processing techniques till the logic scheme for fault confirmation and automated reset. Some simulations are conducted to evaluate the performance of such FPI.**

I. Introduction

Distribution Network Operators (DNO) have been using Fault Passage Indicators (FPI) in Medium Voltage grids as a key element to improve the reliability. These devices have proved to reduce the total outage time by guiding the locating crew straight to the faulted cable section [1]. This time reduction is translated in terms of better SAIDI (System Average Interruption Duration Index) and CAIDI (Customer Average Interruption Duration Index) indexes and also a reduction of the Energy Not Supplied (ENS).

On the other side, manufacturers have made large efforts to reduce the costs associated to the use of this device, in terms of components (reducing the number of sensors, for instance the voltage sensors [2], [3], [4], [5]) but also in terms of time: reduction of the installation time, time required to check the FPI status, time required to reset them and so on [6]. As a result, FPIs are considered a cost effective solution to improve reliability.

The traditional models of FPIs were manufactured as non-directional, since the short-circuit current was assumed to flow from the main grid to the fault location, hence a unique direction. However, the connection of more and more, and larger, Distributed Generation (DG) means that the power flow across the grid is not unique, therefore bidirectional. During faults, DG units also contribute to the fault current, which can be in a reverse direction depending of the fault location and the DG characteristics.

Non-directional FPIs may indicate a fault as forward under reverse current situations. This mal-operation confuses the locating crew, and as a consequence, the fault locating process increases unnecessarily. Some cases of non-directional FPI mal-operation have been identified in [7]. The study shows that the mal-operation is avoided with directional FPIs. Also the back-feed current can lead to mal-trip in non-directional FPIs. This combination of phenomena has triggered the need for directional FPIs, in order to guarantee the high levels of reliability while increasing the amount of renewable energy in the grid.

Such directional FPI can be implemented in the context of an Active Substation, which is fully equipped with voltage and current sensors: the inputs for the implemented device.

In the next sections, the implementation of a digital directional FPI is described in the different levels of complexity. Section II deals with the Medium Voltage (MV) Distribution Network and the fault detection principles, whereas section III describes the polarization and how directional elements work. Section IV describes the signal processing techniques to build the directionality and section V explains the logic scheme that underlies the FPI indication, fault confirmation and reset. Section VI explains the simulations and some results before concluding about the work herein done.

II. MV Distribution grid

For the current application, one of the most important aspects in MV distribution grids is their grounding system. The purpose of earthing the neutral point of the grid is to control and limit the phase-to-ground fault current, hence determining the suitable fault detection methods that can be used. This paper deals with isolated neutral grids, where the neutral point is not earthed.

In the field of FPIs, the most common detection method is the ammetric phase over-current, which implies sensing the phase conductor current of the three-phases. In isolated grids, sensing the phase current allows detecting the following fault types:

- Phase-to-phase faults (about 20-30% of the faults)
- Phase-to-phase-to-ground faults
- Three-phase faults

The thresholds to detect phase over-currents are in the range of 50 A (low trip) to 1000 A, with either definite time or time-current inverse curves, so that the FPI indication is coordinated with the main feeder protections.

However, phase-to-ground faults, the most common type, about 70-80%, cannot be detected by sensing the phase current. In isolated grids, because of the ungrounded neutral point and the low values of the homopolar capacitance of the

cables and overhead lines, the zero-sequence impedance is very high. This implies that the fault current is very small, and in practical terms may be undetectable with phase current sensors. Furthermore, due to the composed error of the 3 phase CTs (Current Transformer), the homopolar current cannot calculated be with (1).

$$3 \cdot \underline{I}_0 = \underline{I}_A + \underline{I}_B + \underline{I}_C \tag{1}$$

For this reason, DNOs that operate isolated grids use a flux summation homopolar CT around the three conductors, so that a more accurate measurement can be obtained.

Concerning the grid voltages, because the grid is not grounded, the ground point can shift and, during a phase-to-ground fault, it displaces to the faulted phase. The line voltages remain as normal values, however the phase voltages increase and shift significantly, in Fig. 1.

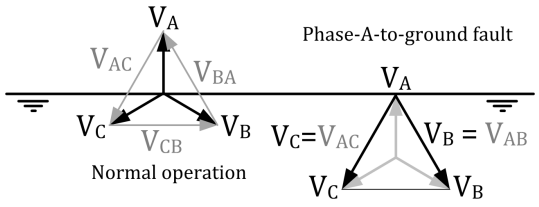

Fig. 1. Phase-A-to-ground fault

The detection of this fault is done by the homopolar over-current, where the current thresholds are abnormally low: in the range of 0.4 to 2 A. As it can be seen in Fig. 1, during fault conditions, the phase-to-ground voltage in phases B and C increases about 73%, and consequently there is a risk of incurring over-voltages, which eventually could derivate in another fault because of break-down of a cable insulation. Therefore, the closest circuit breaker upstream the fault should open as soon as possible to avoid this situation. Consequently, the time margin left to detect the fault is very short: within the order of few electrical cycles.

III. Polarization

The technique of polarization is well known in protective relaying theory. Directional relays work with this technique and have been in use since long time ago. The trip decision is based on the sensed current and the protection curve. The measured current is called the operating quantity and the reference phasor, the polarizing quantity.

The direction decision is taken based on the angle comparison between the operating quantity and the polarizing quantity. It is important to note that the polarizing quantity should remain as stable as possible no matter the current flow direction. Furthermore, it is also required a polarizing quantity ample enough to become a reliable measurement.

For phase-to-phase, phase-to-phase-to-ground and three-phase faults, the quadrature polarization is implemented, whereas for phase-to-ground faults, the zero-sequence polarization is used.

A. Quadrature voltage polarization

The quadrature polarization uses the operating and polarizing quantities of Table I, [8], where $\underline{V}_{CB} = \underline{V}_B - \underline{V}_C$, $\underline{V}_{AC} = \underline{V}_C - \underline{V}_A$ and $\underline{V}_{BA} = \underline{V}_A - \underline{V}_B$.

TABLE I
Quadrature polarization at 90°

Operating quantity	Polarizing quantity
$\underline{I}_A$	$\underline{V}_{POL,A} = \underline{V}_{CB}$
$\underline{I}_B$	$\underline{V}_{POL,B} = \underline{V}_{AC}$
$\underline{I}_C$	$\underline{V}_{POL,C} = \underline{V}_{BA}$

Note that for phase-to-phase faults, even if the faulted phases collapse, the voltage of the healthy phase remains unaffected and is a suitable reference for polarization. The current flow direction is determined by the sign of the "torque" (nomenclature inherited from the traditional electromechanically actuated directional relays) of (2). Positive torque sign indicates a forward fault, whereas negative sign indicates reverse current flow [9].

$$\begin{aligned} T_A &= |\underline{V}_{CB}| \cdot |\underline{I}_A| \cdot \cos(\angle \underline{V}_{CB} - \angle \underline{I}_A) \\ T_B &= |\underline{V}_{AC}| \cdot |\underline{I}_B| \cdot \cos(\angle \underline{V}_{AC} - \angle \underline{I}_B) \\ T_C &= |\underline{V}_{BA}| \cdot |\underline{I}_C| \cdot \cos(\angle \underline{V}_{BA} - \angle \underline{I}_C) \end{aligned} \tag{2}$$

Note that the direction is determined exclusively by the angles of voltages and currents. The forward and reverse regions in the phasor plane for phase A is shown in Fig. 2.

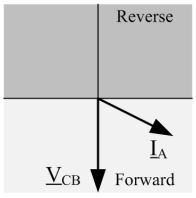

Fig. 2. Forward and reverse regions with quadrature polarization

The quadrature polarization is often complemented with an added fixed angle shift, such as $\pm 30°$, $\pm 60°$ and so on [10], so that the polarizing quantity and the directional decision is adapted to the grid conditions.

Close-in faults is a term used to denote the faults that occur very close to the measurement location, where the three phase voltages can collapse to zero. Using this sequence polarization would not be able to trip because of the non-reliable voltage measurements. In order to overcome this problem, some relays are equipped with polarizing memory ($V_{1,Mem}$), so that when the positive-sequence voltage becomes too low to be accurate, the memory voltage replaces the actual voltage with previous samples [11].

B. Zero-sequence voltage polarization

The zero-sequence voltage polarization uses the operating and polarizing quantities of Table II, and the directional decision is given by (3).

TABLE II
ZERO-SEQUENCE POLARIZATION

Operating quantity	Polarizing quantity
$3 \cdot \underline{I}_0 \cdot (1\angle \underline{Z}_{L0})$	$3 \cdot \underline{V}_0$

Where $\angle \underline{Z}_{L0}$ is the angle of the zero sequence line series impedance. In grounding systems where the homopolar current is mainly active (compensated grounding, for instance), the direction is given by (3).

$$T_{32\text{V}} = |3 \cdot \underline{V}_0| \cdot |3 \cdot \underline{I}_0| \cdot \cos(\angle - \underline{V}_0 - (\angle 3 \cdot \underline{I}_0 + \angle \underline{Z}_{L0})) \quad (3)$$

However, in isolated grids with highly capacitive underground cables, the capacitance of the grid is not compensated with a reactance or a Petersen coil and consequently, the homopolar current is rather capacitive-reactive than active. For that reason, (3) is modified in order to become a better fault indicator, hence calculating the reactive current.

$$T_{32\text{VAR}} = |3 \cdot \underline{V}_0| \cdot |3 \cdot \underline{I}_0| \cdot \sin(\angle - \underline{V}_0 - (\angle 3 \cdot \underline{I}_0 + \angle \underline{Z}_{L0})) \quad (4)$$

Note that in (3) and (4), the zero-sequence voltage angle is in negative so that a positive torque implies forward fault detection.

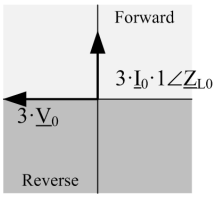

Fig. 3. Forward and reverse regions for a reactive zero-sequence voltage polarization

IV. PROCESSING THE SIGNAL

For the current application, 7 sensors-inputs are considered: 3 phase currents, 1 zero-sequence current and 3 phase-to-ground voltages.

A. Filter

Each input signal needs to be filtered, first to remove noises and second to avoid the high frequency capacitive cable discharge [12]. It has been chosen a cosine *Fourier-notch* filter [13].

$$A_C = \sum_{K=0}^{N-1} f_K(t) C_{AK} \quad (5)$$

$$A_S = \sum_{K=0}^{N-1} f_K(t) C_{BK} \quad (6)$$

Where $f(t)$ is the captured unfiltered sample, K is the number of sample and N is the number of samples per cycle, 16. In a 50 Hz system, the processing frequency is 800 Hz.

The coefficients C_{AK} and C_{BK} are defined by (7) and (8).

$$C_{AK} = (2/N) \cdot \cos(2\pi K/N) \quad (7)$$

$$C_{BK} = (2/N) \cdot \sin(2\pi K/N) \quad (8)$$

The filter frequency response is plotted in Fig. 4.

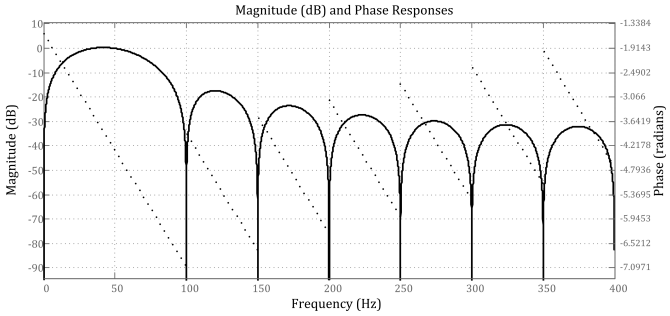

Fig. 4. Frequency response of the implemented filter, at a sampling frequency of 800 Hz

B. RMS calculation

The filtered signal is used for the digital Root Mean Square (RMS) calculation, so that the magnitude of the phasors is already obtained.

$$F_{RMS,t} = \sqrt{\frac{1}{N} \sum_{n=t-N+1}^{t} f_n^2} \quad (9)$$

However, within this implementation, another formula takes the most from the coefficients of the *Fourier-notch* filter, A_C and A_S. These coefficients result in functions such as $A_C = K \sin \omega t$, and $A_S = K \cos \omega t$. Both equations can be combined as:

$$\sin^2 \omega t + \cos^2 \omega t = K^2 \quad (10)$$

Where K is the peak of the sine-filtered signals. The RMS value is obtained:

$$F_{RMS,t} = K/\sqrt{2} \quad (11)$$

C. Internal reference and relative angle

The phase of a signal is calculated between two magnitudes that oscillate at the same frequency. The reference signal can be provided either by a Phase-Locked Loop (PLL) or by an artificial reference, numerically created at the fixed frequency of 50 Hz. Within this implementation the last option is preferred.

Consider the filtered signal as $a(t) = A \cdot \cos(\omega t + \varphi)$ and a reference, expressed in terms of sine and cosine, as $f(t)_{sin,ref} = \sin \omega t$ and $f(t)_{cos,ref} = \cos \omega t$. According to the trigonometric identities:

$$2 \cdot \sin \theta \cdot \cos \varphi = \sin(\theta + \varphi) + \sin(\theta - \varphi) \quad (12)$$

$$2 \cdot \cos\theta \cdot \cos\varphi = \cos(\theta + \varphi) + \cos(\theta - \varphi) \tag{13}$$

Therefore, the multiplication of the references by 2 and by the normalised filtered signal $(a(t)_n)$ leads to an expression that can be split in an oscillating and a non-oscillating term. By calculating the mean of the products, the oscillating terms disappear, leading to terms that only depend on the phase between the original signal and the reference.

$$M_1 = \sin(-\varphi); M_2 = \cos(-\varphi) \tag{14}$$

The phase respect to the reference is obtained by:

$$\varphi = -\tan^{-1}(M_1/M_2) \tag{15}$$

Both coefficients are required in order to preserve the original sign of the angle.

V. Logic scheme

Based on preliminary studies about non-detection cases, it was concluded that the implemented FPI should be able to detect of a second fault while the indication of a previous one might be still on. The operation of the FPI becomes, then, quite complex also because of the DNO requirements, that make use of several counters and simultaneous processes.

The conditions to start indicating a fault are:

- When over-current is sensed, the counter T_1 is activated and starts counting.
- Fault signature logic:
  1) An over-current is detected.
  2) After the fault detection time (*Fault detected*), the main circuit breaker may trip and the line current and voltage fall to zero. The counter T_2 is activated when the fault is detected and the counter starts to count once the absence of current and voltage is sensed.
- The indication of the fault will start only if the counter T_2 finishes before T_1.

The conditions to stop the indication are:

- Manually pressed button. The non-operation of the button can lead to human errors. However, it is a back-up system for any further system.
- Pre-defined reset time (T_4). The FPI switches off automatically after a time of 30min, 1h, 2h, 4h till 24h.
- Electrostatic reset. The FPI understands that when the current/voltage are back to normal levels (above an absence current/absence voltage threshold), the service has been restored and there is no need to keep indicating the fault. The presence of current and voltage needs to be sensed during a time T_3.
- Remote reset signal, sent from the control center to the RTU that may control the communications of the FPI. The mechanism is conceptually similar to the manual button.

The implementation of such set of conditions is done by means of a Finite-State Machine (FSM). The machine remains in one state till a condition triggers it to the next state. During the transition, several actions can take place, finding thus *entry actions* and *exit actions*. The technique is conceptually similar to some heuristic algorithms in loop, that define a unique sequence of facts.

The implemented FSM is formed by 3 states: "normal operation", "waiting for fault detection" and "waiting for fault clearance". The main FSM is in charge of sensing the current and the voltage. Besides this task, it activates several variables that work out of the FSM environment (parallel processes), which control the switch on/off of the indication.

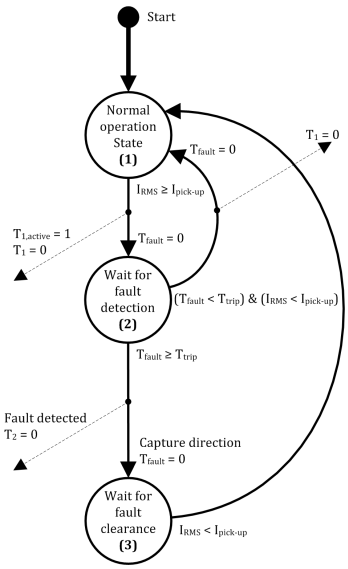

Fig. 5. Main Finite-State Machine (FSM) of the logic scheme proposed for the DNO

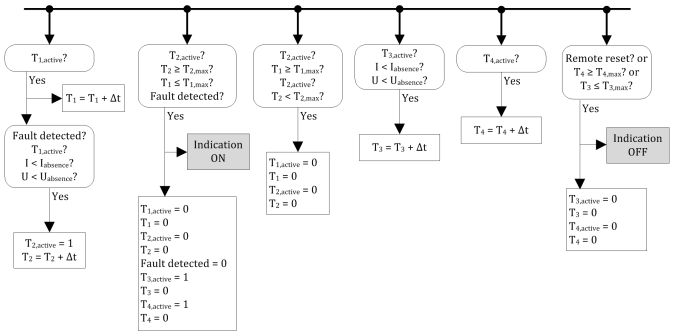

Fig. 6. Parallel processes aside the FSM. Control of the indication ON/OFF. The list of conditions is implemented here

VI. Test and results

In order to evaluate the behaviour of the implemented FPI, an isolated grid has been simulated with several fault types: forward and reverse phase-A-to-ground and phase-A-to-phase-B, with DG. Since the DG units are also operating in isolated neutral mode, they have almost no influence over the zero-sequence current. Furthermore, forward phase-to-phase faults with and without DG are similar between them.

It has been considered that the DG circuit breaker does not follow the main feeder recloser sequence, and therefore, the DG remains disconnected till the service is restored. Except the fault detection timing, the other time thresholds have been adjusted to a shorter time scale in order to reduce the simulation time. Gaussian noise has been added to the signals, with a variance proportional to the sensors pick-up settings. There are 4 FPIs depending on the detection method: FPI-A, FPI-B and FPI-C (for poly-phase faults) and FPI-0 (for phase-to-ground faults). The FPIs indication is normally 'off' (0) and it can take (+1) to indicate forward or (-1) to indicate reverse direction.

A. Implementation platform

The whole system to test the implementation consists of Matlab/Simulink grid, whose parameters are easily controllable externally, so that many parameters can be adjusted: cable lengths, types, fault types, inception angle, DG penetration level amongst many others. This allows to study any scenario in a very short time, only by defining the appropriate conditions. The test grid is plotted in Fig. 7.

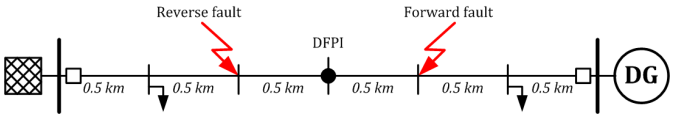

Fig. 7. Test grid

In order to simulate a *real-time* behaviour, the platform runs first the model and stores the signals and the real-time loop is executed then, simulating the reading of the signals as it would happen in hardware.

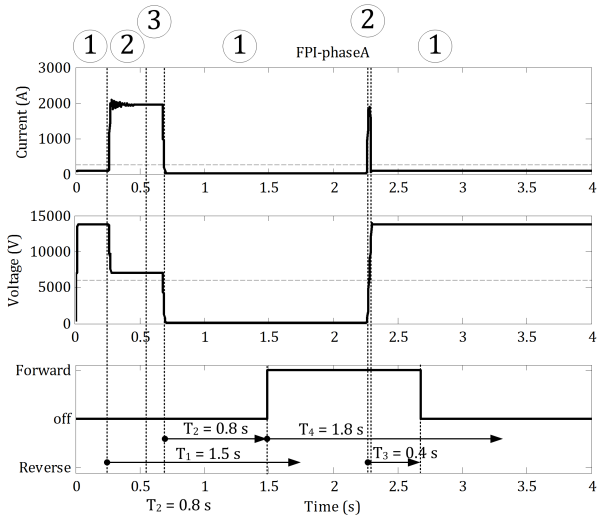

Fig. 8. Forward phase-A to phase-B fault chronograph. The different states of the FSM and the counters described in section V are drawn. Up: phase-A current. Middle: phase-A to ground voltage. Down: FPI-A.

By conducting several simulations some relevant cases have been found. These will be describes in the next subsections, classified depending on the issue.

B. Detection problem

The reported problem is well known for the DNOs that operate isolated neutral grids and overhead lines. During phase-to-ground faults, the total zero-sequence impedance of the grid very large because of the capacitance of the overhead lines. This leads to a very small zero-sequence current, that often can barely be sensed by the summation CTs. This scenario has been simulated with a self-extinguishing and a permanent fault when the circuit breaker is operated with a recloser. Recall the small values of zero-sequence current, which in practice imply FPIs with very low settings (between 0,4 and 2 A) to detect this fault type.

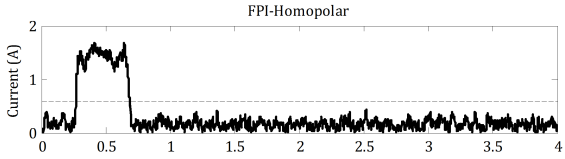

Fig. 9. Zero-sequence current during a self-extinguishing phase-A to ground. Note that when the recloser reconnects the fault has disappeared and therefore there is no fault to indicate. The FPI does not detect absence of current and voltage.

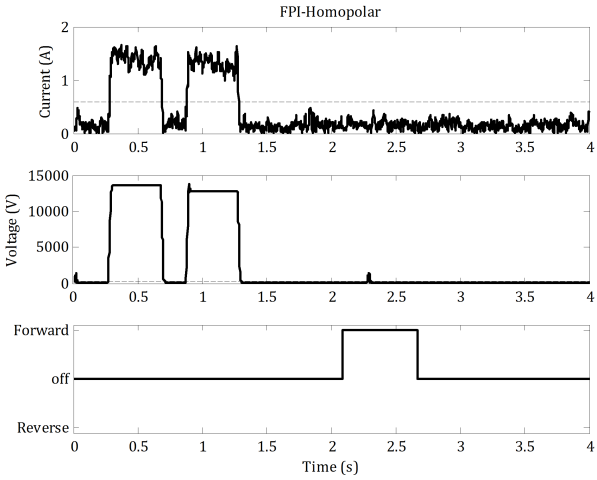

Fig. 10. Zero-sequence current during a permanent phase-A to ground.

Like in Fig. 8, the indication starts after sensing absence of current and voltage during 1,8 s after the fault clearance.

C. Directional problem

A directional problem was found when analysing a phase-B to phase-C fault and an increasing fault resistance. The forward region for this fault type is driven by the phasor $\underline{V}_{AC}$, as shown in Fig. 11. These simulations are carried out with underground cables.

This case justifies the use of the angle shift in the quadrature polarization, as mentioned in section III, so that the fault current falls always inside the forward region, ensuring the right direction detection. The most common angle shift is -30°,

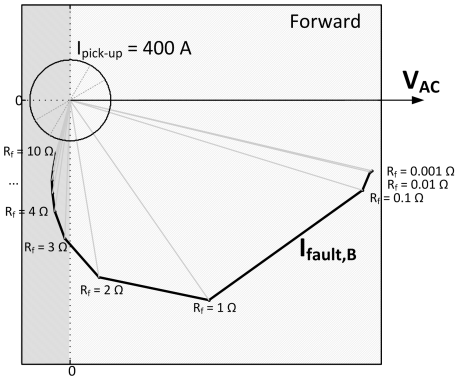

Fig. 11. FPI-B phasor diagram with polarization regions (forward/reverse) for a forward phase-B to phase-C fault with increasing fault resistance. Note that the phase-B current phasor moves towards the reverse region with the increasing fault resistance.

which implies a clockwise rotation of 30°of the directional regions. However, in [14], the angle shift can also be set up as the angle of the positive-sequence line impedance ($\angle \underline{Z}_{L1} = 34.93°$). Other possibilities such as -60°or -90°are also possible.

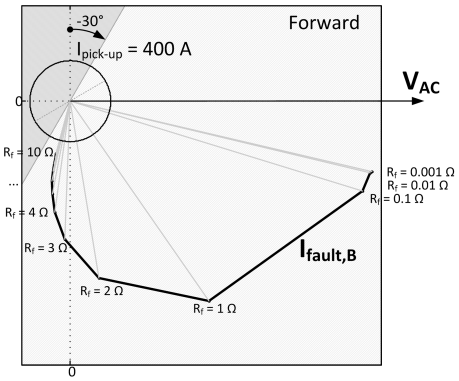

Fig. 12. FPI-B phasor diagram with polarization regions (forward/reverse) for a forward phase-B to phase-C fault with increasing fault resistance with a phase shift of -30°.The phasor falls now inside the forward region.

VII. Conclusions

This paper presents a vertical approach to the directional fault detection problem and procedure. The paper describes the steps from the signal processing to the grid topology and its operation, formulated in terms of logic actions. Isolated neutral grids is a special case because of the low fault currents, which requires the use of zero-sequence measurements and a specific polarization method.

The implementation of such directional FPI has been done in Simulink, with digital techniques. This platform allows to build complex systems to improve the performance of the device, concerning the coordination with the main feeder protection and the circuit breaker operation. In that sense, there exists a difference in time between the fault detection instant and fault indication instant, which is due to the implemented logic scheme, that enables some features such as the fault signature with recloser or the electrostatic reset.

The platform for FPI testing has been built flexible enough to allow the fast creation of a faulty scenario so the FPI performance can be checked beforehand in a wide variety of scenarios. The tests show a proper behaviour of the implemented directional FPI concerning the response to the logic scheme, which is coherent in terms of timing.

Furthermore, by simulation, some potential mal-operation cases are recognized. The first one concerns the zero-sequence fault current detection. The scenario has been modelled realistically so that the real problem of low currents can be observed. The second mal-operation case concerns phase-to-phase faults, where a directional problem has been identified when high resistance faults happen. The technique of shifting the forward/reverse regions has been proved to be effective and easily implementable, without influence or with improvement in direction detection of other faults with high impedance, such as phase-to-phase-to-ground faults.

Acknowledgment

This work has been funded by the KIC-InnoEnergy Active SubStations project. The authors thank the kind contributions from Eva Alvarez González and Miguel García Lobo, from Gas Natural Fenosa.

References

[1] E. Vidyagasar, P. V. N. Prasad, and A. Ather Fatima, "Reliability Improvement of a Radial Feeder Using Multiple Fault Passage Indicators," *Energy Procedia*, vol. 14, p. 1, Jan. 2012. [Online]. Available: http://linkinghub.elsevier.com/retrieve/pii/S1876610211043037

[2] C. González, T. De-Rybel, and J. Driesen, "Enhancing reliability in medium voltage distribution networks with directional fault passage indicators without voltage sensors." Unpublished, 2013.

[3] Abhisek Ukil and Bernhard Deck and Vishal H. Shah, "Current-Only Directional Overcurrent Relay," *IEEE Sensors Journal*, vol. 11, no. 6, pp. 2010–2011, 2011.

[4] G. Verneau, Y. Chollot, and P. Cumunel, "Auto-Adaptive Fault Passage Indicator with Remote Communication Improves Network Availability," in *CIRED*, no. 0245, 2011, pp. 6–9.

[5] P. Cumunel and G. Verneau, "Identification and directional detection of a defect in a three-phase network, European Patent EP 2383856," 2011.

[6] F. M. Angerer, "New Developments in Faulted Circuit Indicators Help Utilities Reduce Cost and Improve Service," no. 08, 2008, pp. 0–3.

[7] C. Andrieu, B. Raison, D. Penkov, M. Fontela, S. Bacha, and N. Hadjsaid, "CRISP - Fault detection , analysis and diagnostics in high-DG distribution systems," Tech. Rep., 2004.

[8] J. Roberts, N. Fischer, and B. Fleming, "Obtaining a Reliable Polarizing Source for Ground Directional Elements in Multisource, Isolated-Neutral Distribution Systems," Schweitzer Engineering Laboratories, Tech. Rep.

[9] J. Roberts, D. H. Altuve, and D. D. Hou, "Review of Ground Fault Protection Methods for Grounded, Ungrounded and Compensated Distribution Systems," Schweitzer Engineering Laboratories, Inc., Tech. Rep.

[10] Troy D. Graybeal, "Factors Which Influence the Behavior of Directional Relays," *AIEE Transactions*, 1942.

[11] Z. N. Stojanović and M. B. Djurić, "The algorithm for directional element without dead tripping zone based on digital phase comparator," *Electric Power Systems Research*, vol. 81, no. 2, pp. 377–383, Feb. 2011.

[12] Cooper-Power-Systems, "Faulted Circuit Indicator Application Guide," Cooper Power Systems, Tech. Rep. October, 1998.

[13] W. A. Elmore, *Protective Relaying Theory and Applications*. CRC Press, 2003.

[14] J. Roberts and A. Guzman, "Directional element design and evaluation," Schweitzer Engineering Laboratories, Inc., Tech. Rep., 2006.